Res. Rep. Fac. Eng. Mie Univ., Vol. 25, pp. 1 −15 (2000)

Original Paper

Quantifying carbide particles in steel by image processing method

Hiroshi KAWAKAMI, Koreaki TAMAKI and Kanta TAKAHASHI
(Department of Mechanical Engineering)

(Received September 18, 2000)

Abstract

SR embrittlement arises in HAZ of 2 1/4Cr-1Mo steel by the long-time reheating in SR treatment. The behavior of carbide particle seems to have close relation with SR embrittlement, as they grow significantly in the time range of SR embrittlement. The number of carbide particles which observed on the fracture surface of the specimen suffered from SR embrittlement is larger than that in cross-section. The systematic investigations may be needed to discuss the role of carbide particles on SR embrittlement. In this study, the size and shape of carbide particle were measured systematically by using the image processing. The experimental system for quantifying of carbide particles is combined with scanning electron microscope (SEM) and a personal computer. The suitable method of image processing which can recognize the shape of carbide particles in the image by SEM was established in the fast place. The size of carbide particle in cross-section increased with an increasing time of SR treatment. The shapes of carbide particles in cross-section changed from sphere to elliptical with the growth of particle. But the relation between the size and shape of carbide which was observed on fracture surface was different from that in cross-section when SR embrittlement occurs significantly. The fractured carbide particles were observed on fracture surface. This result suggests that the crack propagation in carbide particles helps to occur SR embrittlement.

Key words : image processing, shape of carbide particle, SR embrittlement, SEM image, 2 1/4Cr-1Mo steel, cleavage fracture.

1. Introduction

Weldments made of heat-resisting Cr-Mo steels are usually stress-relieved after

welding in the temperature range around 975K [1]. When the time for stress-relieving (SR) treatment exceed 10h, the notch-toughness in the heat-affected zone (HAZ) is reduced significantly. This phenomenon is named SR embrittlement [2,3]. The carbide particles in steel seem to play an important role to cause SR embrittlement, as they grew in large scale with the lapse of holding time at 975K [4,5].

The object of this study is to confirm the direct relation between the carbide particles of large scale and the SR embrittlement.

The quantitative analysis of carbide particles in steel involves (1)the SEM observation, (2)the measurement of each size of particles and (3)the measurement of the number of particles in an unit area [6]. However, latter two items require long time to get enough accuracy of the result when it carried out by the manual process. The image processing is now applied widely to inspect the products in manufacturing systems. With this computerized technique, a product is investigated for its shape easily by recognizing it as a digital image. If this image processing can be applied for this study, enough data will be given in a short time.

In this study, the image analysis method which recognizes carbide particles in SEM image was established by the combination of some kinds of image processing and carbide particles in cross-section or on fracture surface of specimen were quantified.

2. Background of this study

The SR embrittlement was detected by the rise of the transition temperature vTr_{30} (the temperature which gives the absorbed energy of 30 ft-lb). The transition temperature begins to increase from 7h (the point S_{SR}) at 975K as shown in Fig.1(a). The average size and number of carbide particles which were measured by the manual process are shown in Fig.1(b) and (c). The average size for the carbide particles existing in the cross-section of the specimen, their average

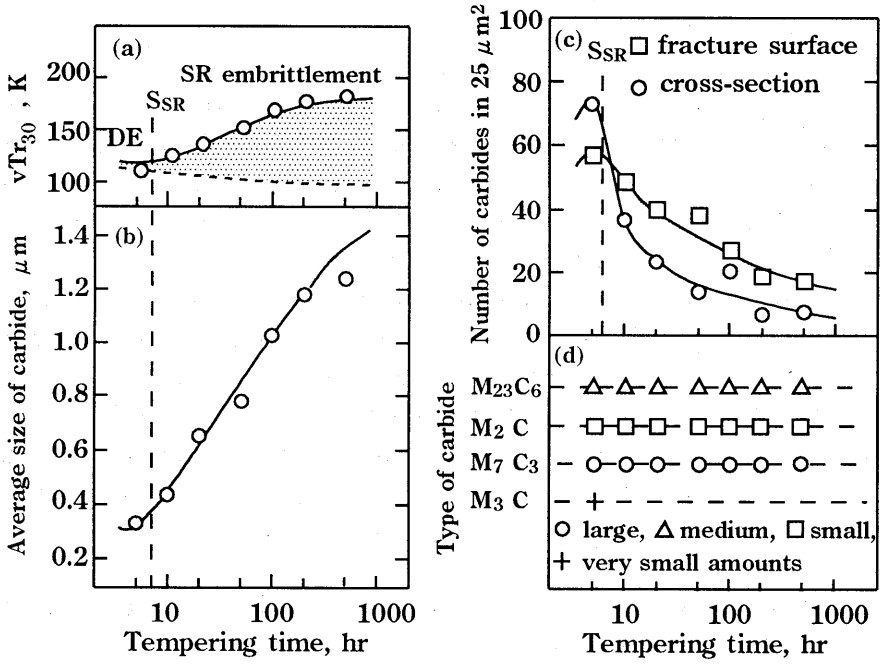

Fig.1 Change in size and number of carbide particles in the time range of SR embrittlement; (a)transiton temperature, vTr30, (b)average size of particles, (c)number of particles in cross- section and on fracture surface, (d):types of carbide detected by X-ray diffraction.

size increases and their number is decreases from the time S_{SR}. The number of carbide particles was also measured on the fracture surface of specimen which was fractured at 125K; the fracture exhibits the cleavage type. The number of particles is larger for the fracture surface than for the cross-section in all time range where the SR embrittlement arises as shown in Fig.1(c). The types of carbide particles existing in the time range of SR embrittlement are $M_{23}C_6$, M_2C and M_7C_3, respectively (Fig1(d)).

These results suggests that the growth of carbide particles will be the major cause of SR embrittlement.

3. Experimental system

3.1 Specimen

The synthetic HAZ specimen of 2 1/4Cr-1Mo steel in which the microstructure of the real HAZ was reproduced, was prepared [5]. The specimens were tempered at 975K, for 5 to 500h. They were fractured by Charpy impact test at the temperature below the transition temperature. The specimen was fractured with very low absorbed energy producing the cleavage type fracture. The fracture surface and cross-section of each specimen were etched by 3% nital to reveal the contours of carbide particles. The etching temperature and time are 293K and 40s.

3.2 Image processing system

The image processing system which was used in this experiment is composed with Scanning Electron Microscope (SEM) and a personal computer. The image in CRT of SEM is forwarded to the personal computer as the original image for the image processing. Forwarding of the original image and image processing were carried out on the original image by SEM image filing system Db-sem III. The sizes of carbide particles in one image after image processing were measured by automatic measurement function.

4. Construction of image processing

Globular carbide particles are normally observed in the microstructure of the tempered carbon and low alloy steels. Carbide particles are usually small in size are dispersed in ferrite matrix, even though the specimen is tempered at 975K for a long time as shown in Fig.1(b) and (c). In this chapter, the some method of image processing which were assembled some kinds of image processes were investigated to recognize a number of carbide particles in one original image.

4.1 Preprocessing

4.1.1 Feature of carbide particle in the original image

Fig.2 shows two original images of carbide particles. The image A shows the original image in which some carbide particles on cleavage fracture surface exists by a magnification of 30000 (Fig.2(a)). The large carbide particle which exists in center portion in the frame of image A is named particle A. Image B shows the original image in cross-section by a magnification of 10000 (Fig.2(b)).

The brightness of each carbide particle in the original image A and B is different each other. The difference of brightness of each particle in image A which was taken on fracture surface is more remarkable than image B. The difference of brightness may be caused by the difference of types of carbides and the height of the existence location. The effect of difference of brightness of particles on image processing was investigated by using image A in this section,

because the difference of image A is grater than that of image B.

The sequences of type I-A and I-B image processing show as follows.

Type I-A: Binarization→Closing→Median filter

Type I-B: Brightness&Contrast→Closing→Median filter.

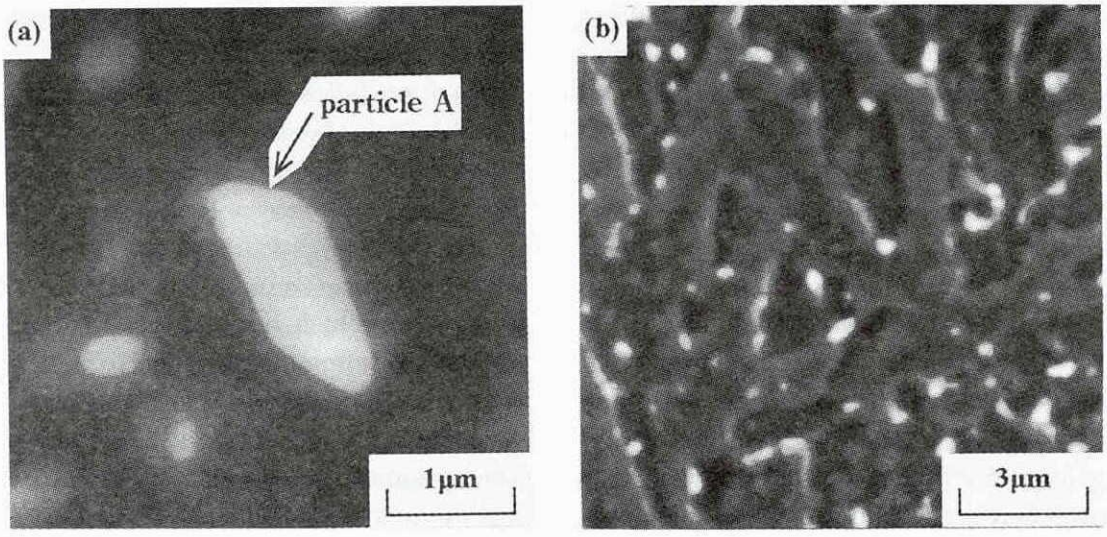

Image A Image B

Fig.2 Original images of carbide particles used for the image processing; (a)image on fracture surface, (b)image in cross section of specimen.

The binarizaton is the process which transforms the original image to binary image. The brightness&contrast is the process which adjusts the brightness and contrast of original image to make a clear image. The dilation is the process in which the layers of pixels are added on the peripheries of particles. The erosion is the process in which the layers of pixels are removed from the peripheries of particles. The closing is the process which assembled dilation was carried out after erosion. It is used to fill holes within particles or to smooth edges of particles. The median filter is used for removing high frequency noise[7].

Fig.3(a) shows the final image by the type I-A image processing. When binarization was carried out, the threshold value was determined to fit the edge of particle A of the original image. The area of this particle was same as that obtained by visual operation on the original image as shown in Table 1. However, the other particles which exist in the original image disappeared or deformed by binarization, because the threshold values of other particles except for particle A are different from a suitable one of the particle A. The difference of brightness of each carbide particle causes the imperfect result. It is difficult to recognize a number of particles in one image by binarization.

Fig.3(b) shows the final image obtained by the type I-B image processing. The adjustment of brightness was determined to fit the brightness value at the edge of carbide particle A of the original image and that of contrast was maximum to clear the edges of particles. A few carbide particles with the particle A were recognized by this method of image processing. The area of the particle A by type I-B processing as shown in Table 1 was larger than that by visual measurement. The brightness&contrast may be a useful preprocessing for the plural particles in one original image, but it is difficult that all particles in one original image are recognized sufficiently by a blanket preprocessing in type I-B image processing.

4.1.2 Image dividing

In order to recognize the plural carbide particles in SEM image, it is necessary to modify the preprocessing by brightness&contrast as shown in 4.1.1. Preprocessing using image

dividing was investigated as follows. The original image is divided into the adequate size for preprocessing. The particles in each divided part were processed by the brightness&contrast adjustment. After that, each divided part was aligned to the original size.

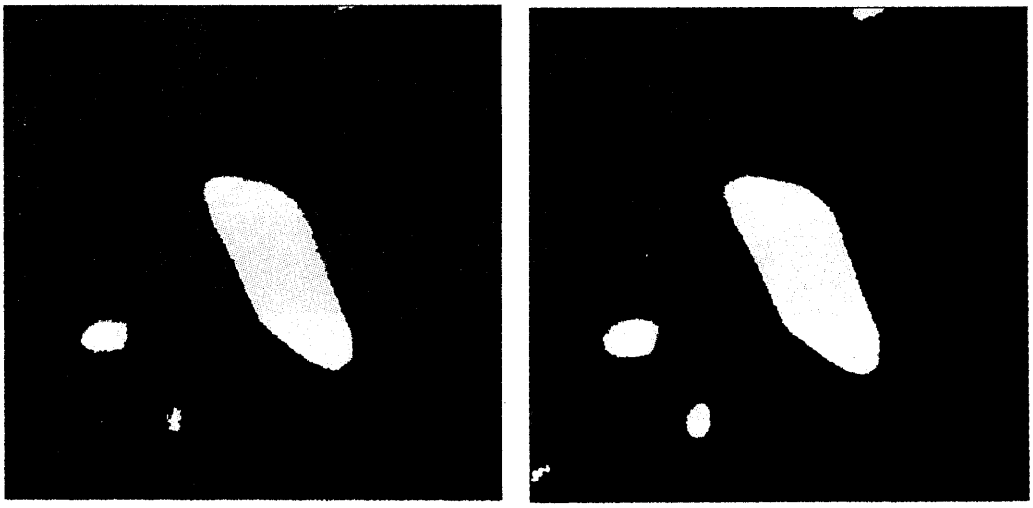

(a)Type I-A (b)Type I-B

Fig.3 The final images which were obtained by type I-A and I-B image proccesing on the original iamge A.

Table 1 Area of particle A measured by five different methods.

Type of measurement	Area of particle A (μm^2)	Difference ratio from visual measurement (%)
Visual measurement	1.032	——
I-A image processig	1.034	0.19
I-B image processing	1.135	9.98
II-A image processing	1.035	0.29
II-B image processing	1.037	0.48

4.2 Image processing

The carbide particles in original image are analyzed by image processing after preprocessing. Some methods of image processing were investigated systematically.

The sequences of the type II-A and II-B image processing show as follows;

Type II-A: preprocessing→Erosion→Opening,

Type II-B: preprocessing→Opening→Erosion.

Opening is the assembled image processing in that erosion is carried out after dilation. It is used to separate the particle without unwanted features [7].

The areas of particle A in image A by each image processing is compared in Table 1. The area by two methods are same as visual measurement. The measurement value for the area of particle A by type II-A image processing improved slightly than that by type II-B. The progression of images processing during type II-A image processing shows in Fig.4.

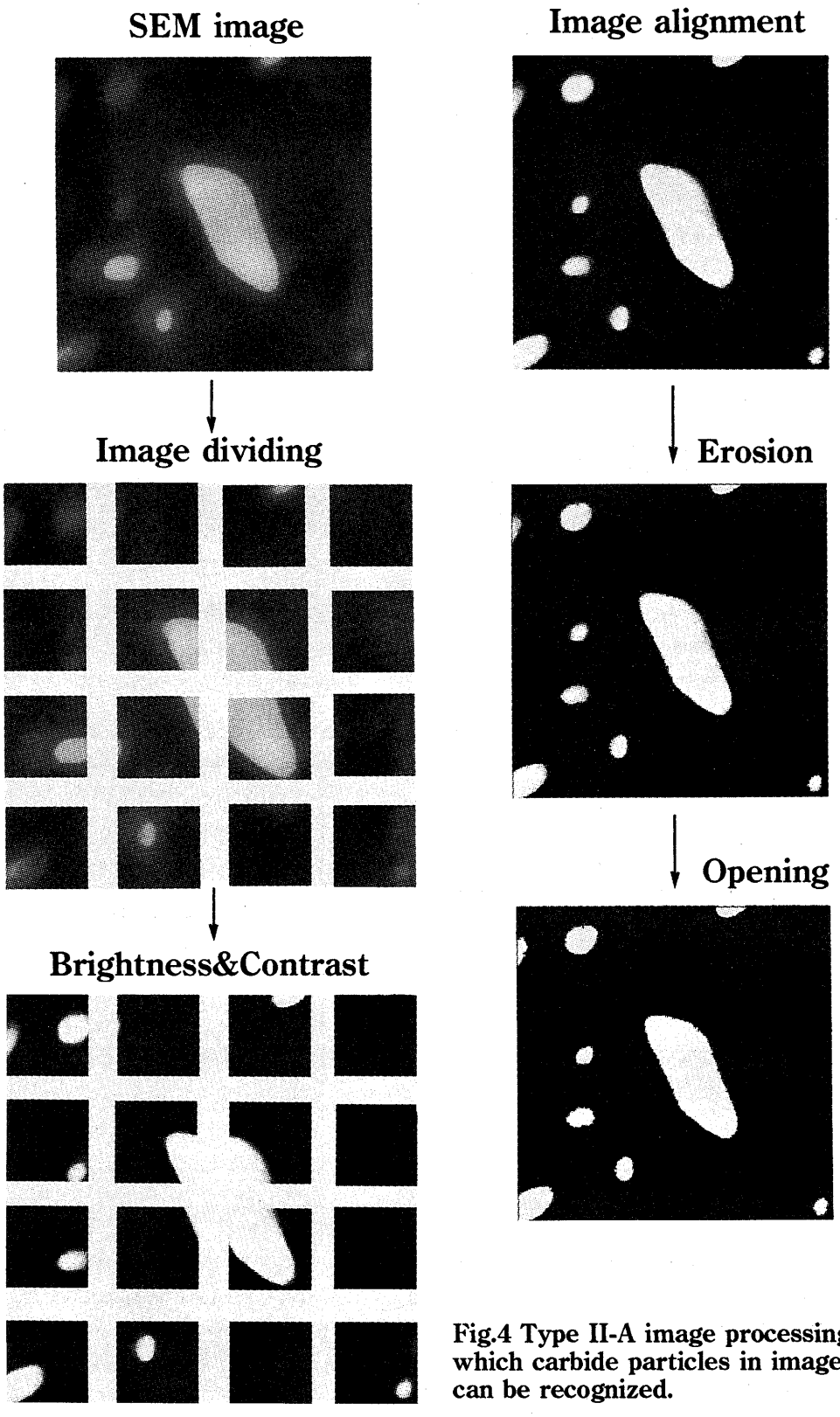

Fig.4 Type II-A image processing by which carbide particles in image A can be recognized.

The results of the area of carbide particles in image B which were obtained by visual and auto measurement show in Fig.5. These measurements were carried out by several types of image dividing.

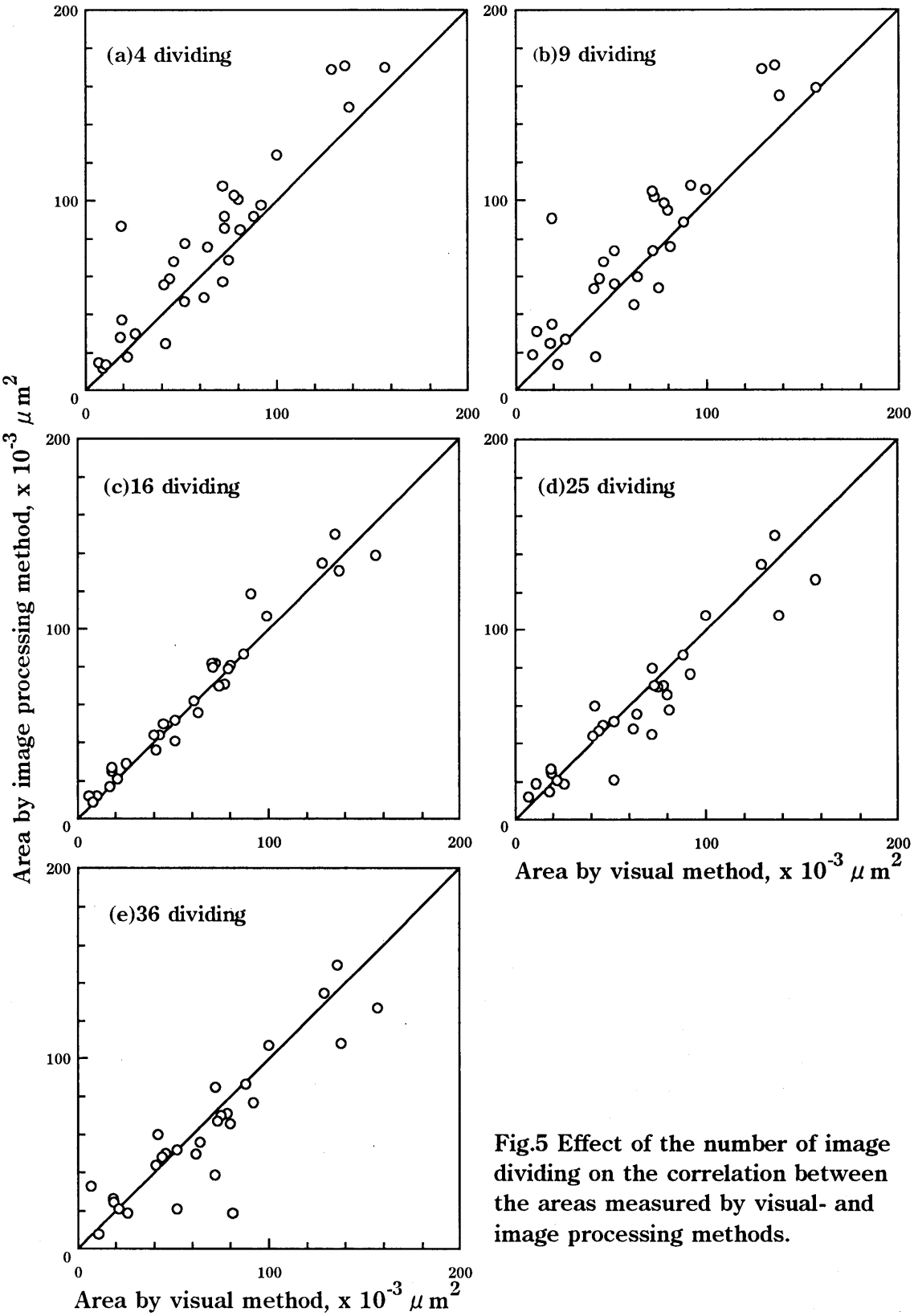

Fig.5 Effect of the number of image dividing on the correlation between the areas measured by visual- and image processing methods.

The areas of carbide particles by auto measurement with the image dividing into less than 16 increased generally than the ones by visual measurement. In this case, the areas of the bright particles in each image part increased, because the brightness were adjusted to fit to low brightness of the faint particles (Fig.5(a) and (b)). In case of the dividing into 16, the result shows that the area of each particle which was measured by each method has a good correlation (Fig.5(c)). However, the areas obtained by image processing with more fine image dividing than 16 dividing decreases generally. The outline of particle existing near the frame line of image part is not clear, because they were broken by fine image dividing (Fig.5(d) and (e)).

From these results, type II-A image processing with 16 image dividing was used to quantify for the size and the shape of carbide particle in the following chapter.

5. Quantifying of carbide particle

5.1 Parameters for measurement

The following parameters were measured to quantify for the shape of carbide particles in cross-section and on fracture surface of the specimens which were tempered at 975K . These parameters shown in Fig.6 are as follows,

R: The radius of the outer circle when the center of mass of the particle is placed at the center of the circle.

R': The radius of inner circle.

R/R': The ratio of R and R'.

R/R' of the circular particle is 1. R/R' exceeds 1 for the case of the spindle particles.

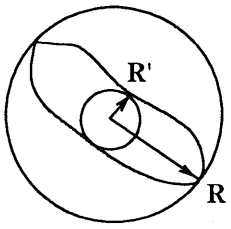

Fig.6 The diagram for maximum radius R and minimum radius R of carbide particle.

5.2 Measurement in cross-section

5.2.1 Distribution of maximum radius

The image processing method was applied for measuring the maximum radius of each carbide particle in a image frame selected randomly. The magnification was changed from 15000 to 5000 in order to hold the whole shape of a carbide particle in one image part.

Fig.7 shows the distributions for maximum radius R of carbide particle. In short time range of SR treatment, only fine particles existed. The peak of number appears at 0.1 μ m (Fig.7(a) to (c)). Mean R increases with the lapse of holding time at 975K. The distribution of R becomes broad in shape in the long time range and the distribution becomes asymmetrical in shape. The particles which are larger than mean R are observed. For the holding for 500h, the coarsened carbide particles, as large as more than 1 μ m, were observed. This result shows the coarsening of carbide particles by excess SR treatment [5]. Even in this case, fine particles as small as 0.1 μ m, were still observed (Fig.7(d) to (g)).

The distribution of R is plotted against the holding time as Fig.8. Sakuma et al. investigated the radius of carbide particles of a quenched Cr steel against the tempering time at 975K [8]. The radius increased with the holding time at 975K. Their results show as the dotted line in this figure. The maximum values of R increases with an increasing time. The minimum of R did not change in all the time range. The minimum values of R in the long time range are very small than the radius which is shown by the dotted line. This result shows that the precipitation of fine carbide particles continues to occur in the time range as long as 500h.

5.2.2 Difference between average size and mean R

The average size of carbide particle, which is the length of the major axis of an elliptical particle [5], was shown in Fig.1(b). The mean R should theoretically meet half of the average size, however, they do not meet in practical as shown in Fig.7. The former is smaller than the latter. The difference tends to increase with an increasing with an increasing holding time.

For the case of the average size, the measurement was carried out on particles of all the sizes in the specimen [5]. A half value of average size shows mean value of the range of R. The other side, mean R shows mean value of all the particles which were observed. Because mean R contains the values of coarsened carbide particles and fine one which precipitated newly by SR treatment, it shows the radius which shows the peak of each distribution. It may be better to discuss on the average size of carbide particle when the behavior of the growth of carbide particles by SR treatment shows than mean R.

5.3 Measurement on fracture surface

Fig.9 shows the distributions of R of carbide particle existing on the fracture surface. Referred to the histogram of Fig.7, it is seen that the number of particles in the R class greater than the mean R is larger for the fracture surface than for the cross-section. The large carbide particles (for example, R class of 0.5 μ m) which could not be observed in the cross-section by this experiment were observed in short time range. The increase of maximum radius, R is shown in Fig.10. The mean R for the fracture surface (the solid circle) is larger than for the cross-section (the dotted line) in all the time range. These results in Fig.9 and 10 suggest that coarse carbide particle is major cause of SR embrittlement. The maximum value of R on fracture surface increased with time of SR treatment. However, this value in the fracture surface it is very smaller than that in the cross-section (Fig.7).

6. Discussion

The relation between maximum radius R and the ratio R/R' is shown for the specimen held for 500h at 975K as in Fig.11. The data in cross-section and on fracture surface are shown by the solid circle and open circle, respectively. In case that the R is smaller than 1.0 μ m, the ratio R/R' increased with an increasing R. The carbide particle becomes elliptical in shape with an increasing holding time. In case of the R larger than 1.0 μ m, the coarsening of carbide particles classified into two modes. In the first mode, the ratio R/R' of particle increases with an increasing of R. In this mode, carbide particle grows unidirectionally to form an elliptic particle. In second mode, the ratio R/R' remains a constant value during coarsening. In this mode, carbide particle will grow tridirectionally as the shape is kept the original shape. Some of them will be coarse by combination with the neighbor particles.

The maximum value of R on fracture surface is smaller than that in cross-section. In case of the R smaller than 0.5 μ m, the ratio R/R' on fracture surface is same as that in cross-section with the same R (Fig.11). This result suggests that the carbide particle was not fractured when the specimen was fractured in the crystal plane on which this carbide particle existed. The crack propagates along the interface between carbide particle and ferrite.

In case of R larger than 0.5 μ m , the ratio R/R' is large for the fracture surface for the cross-section with the same R. This result suggests that long elliptical carbide particle was cut and separated into more than two pieces when the specimen was fractured.

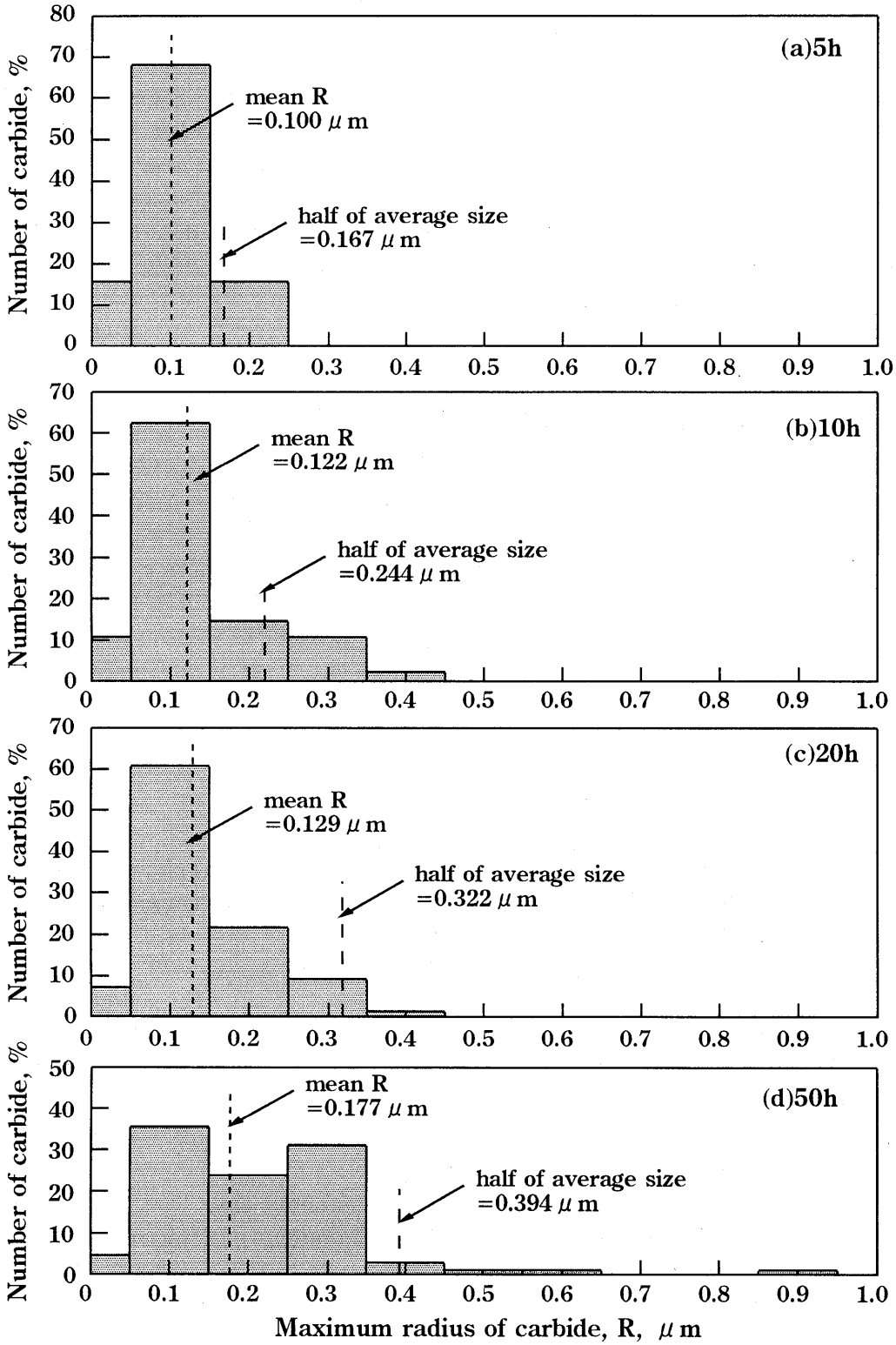

Fig.7 Distribution of maximum radius of carbide particles, R observed in cross section of each specimen.

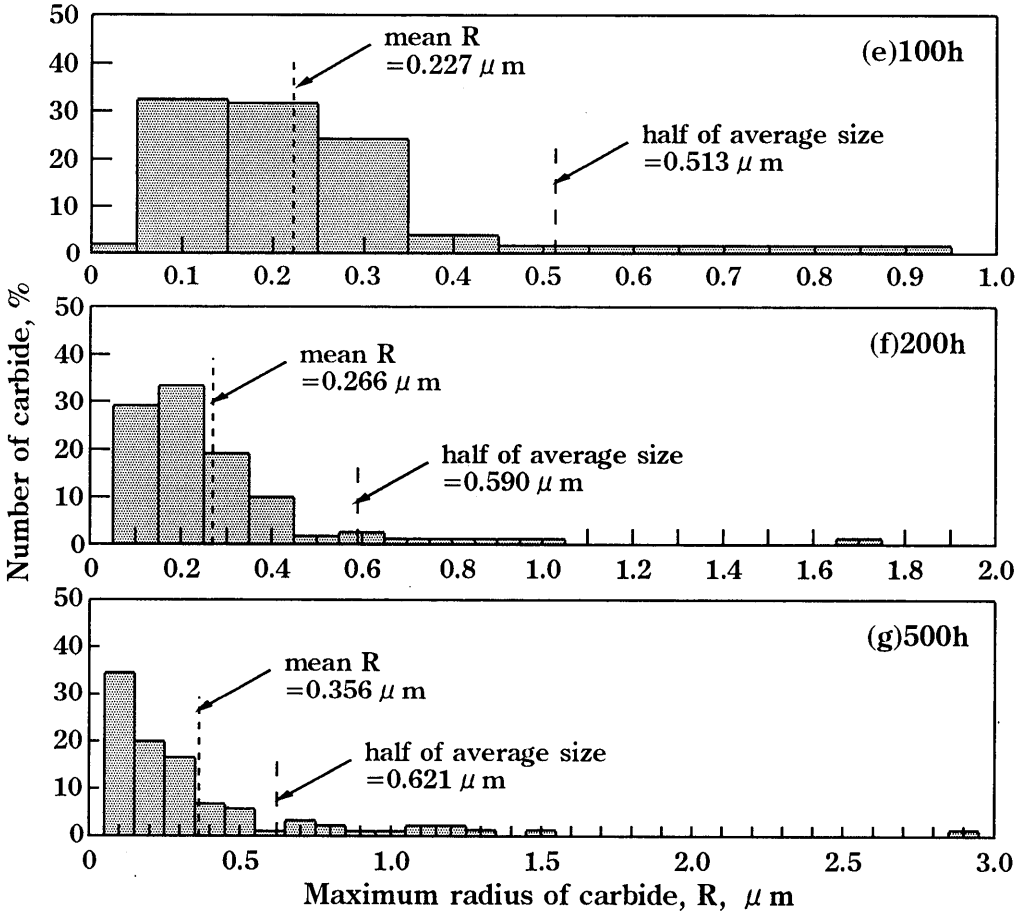

Fig.7 Continued.

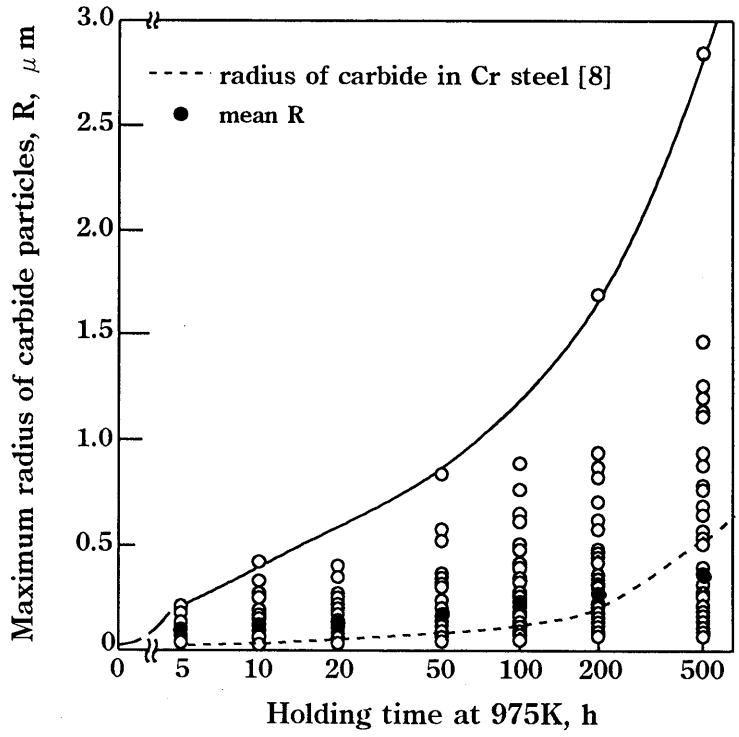

Fig.8 Increase of the maximum radius of carbide particle, R with increasing holding time at 975K; cross-section.

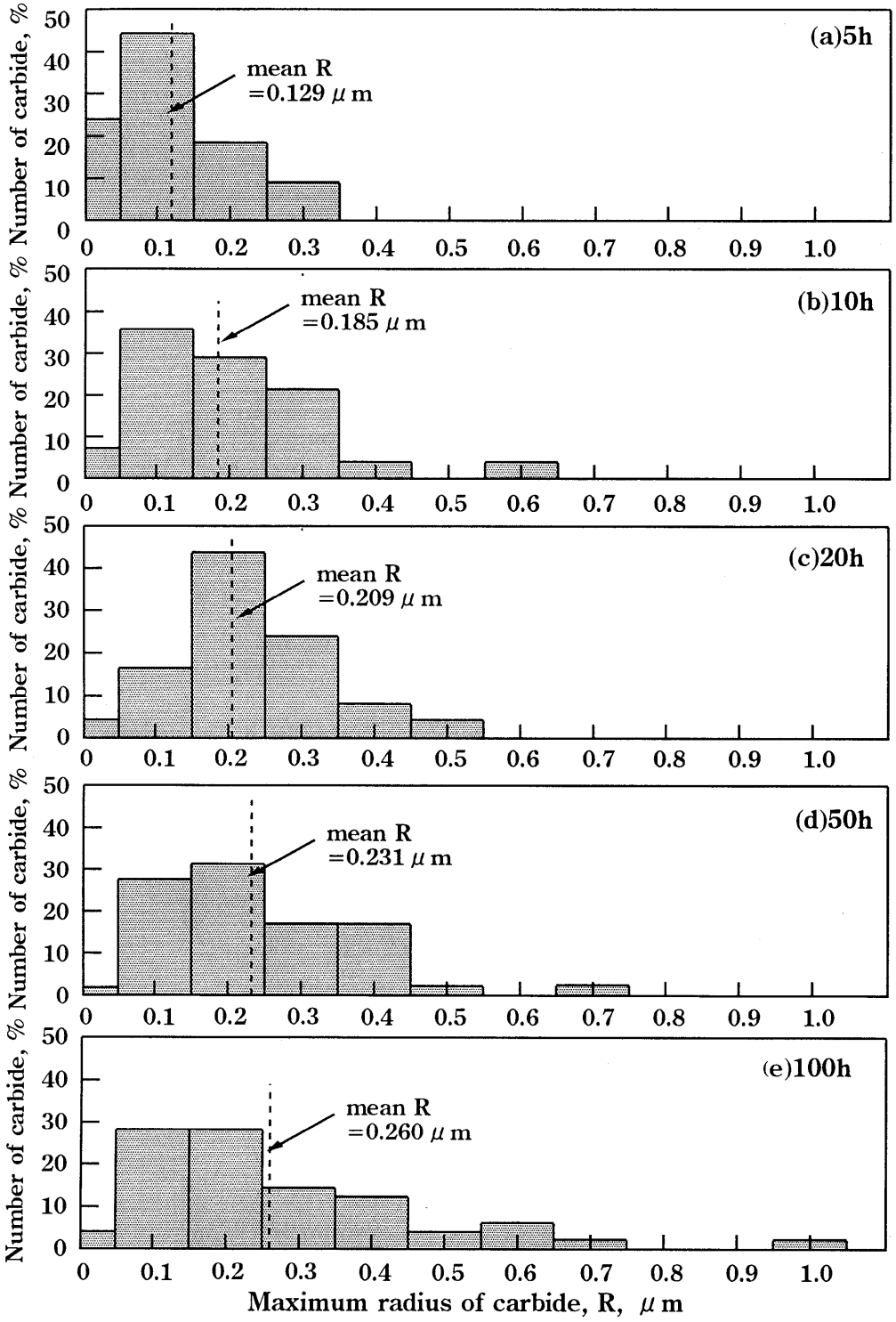

Fig.9 Distribution of maximum radius of carbide particles, R observed on fracture surface of each specimen.

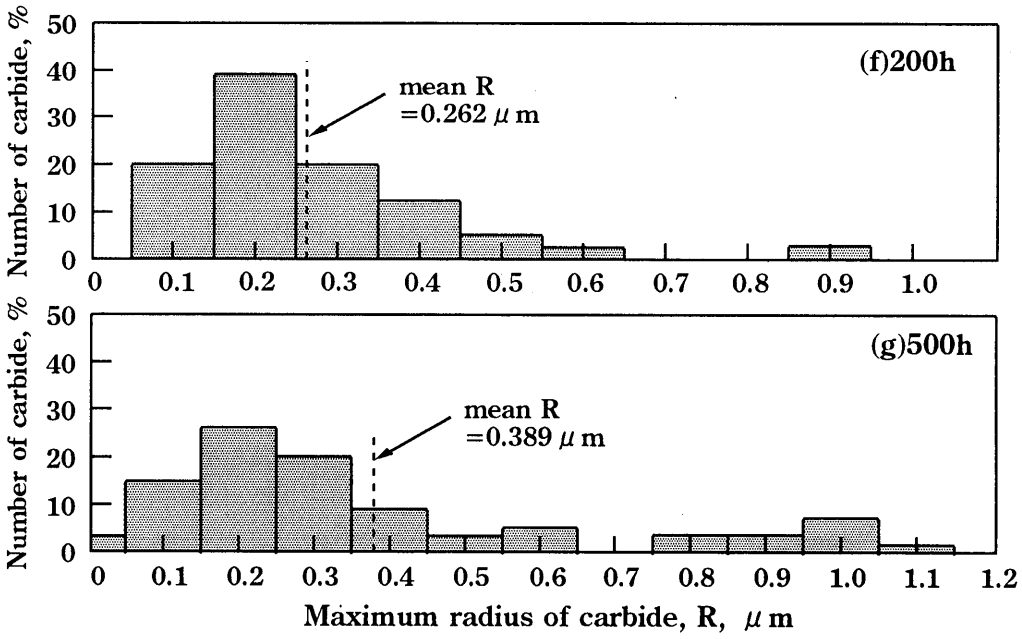

Fig.9 Continued.

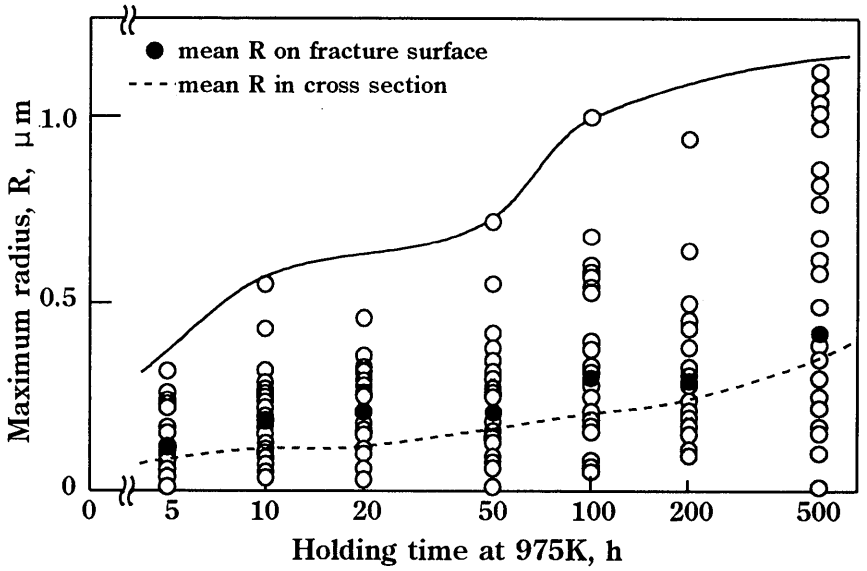

Fig.10 Increase of the maximum radius of carbide particle, R with increasing holding time at 975K; fracture surface.

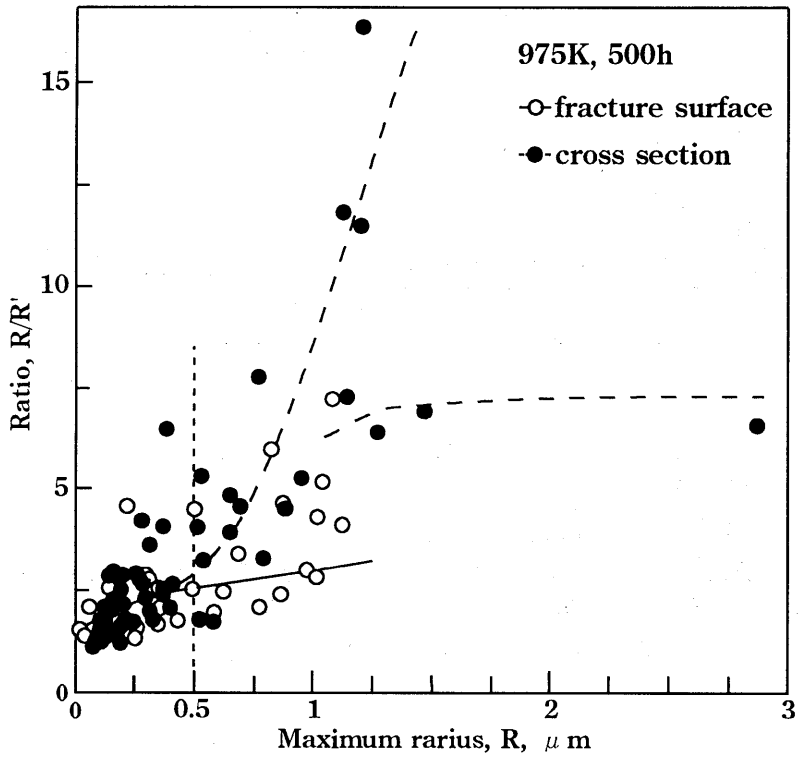

Fig.11 Relation between R/R' and R of carbide particles observed in cross section and fracture surface.

A pair of fracture surfaces of a specimen is shown in Fig.12. In this case, one carbide particle was separated into three parts; the parts A and C were left on one fracture surface (left) and the part B was left on another fracture surface. Coarsened carbide particles will cause SR embrittlement by preparing the site at which the cleavage fracture is initiated. The separation of coarsened carbide particle may occur at the combined part with the other particles.

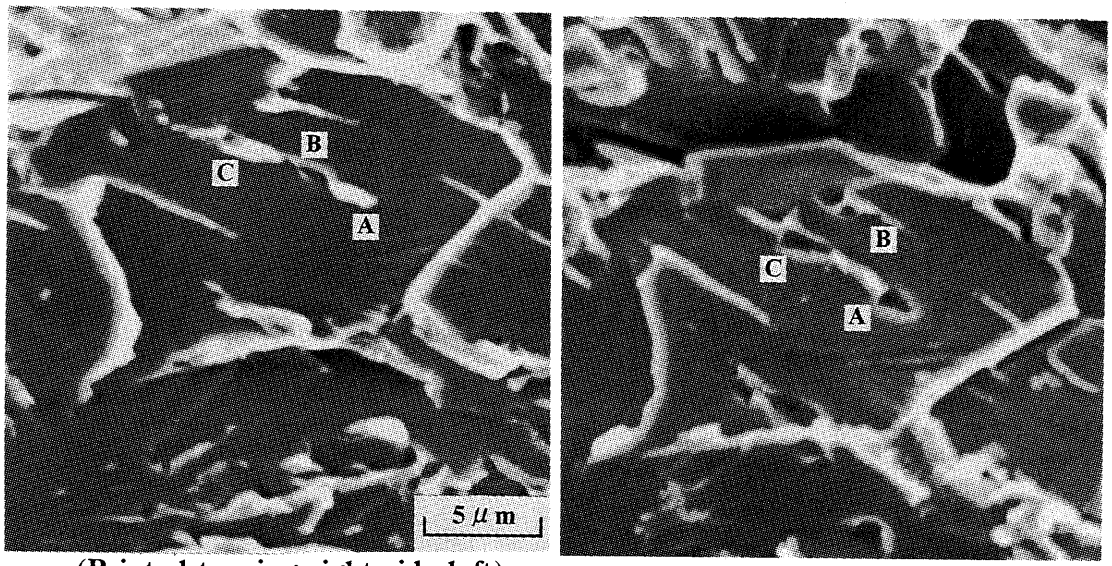

(Printed turning right side left)

Fig.12 Carbide particle which was cut by into three pieces on a pair of fracture surfaces.

7. Conclusion

Effect of carbide particles on the SR embrittlement was discussed by using the experimental technique of the image processing on the particles.

(1)The shape of carbide particle in SEM image was recognized by the following image processing.

Image Dividing→Brightness&Contrast→Image Alignment→Erosion→Opening

(2)Fine carbide particles were observed in the long time range. This shows new carbide particles precipitated by SR treatment.

(3)The carbide particle grows with an increasing time of SR treatment. The coarsening of carbide particle occur with two modes. One is the coarsening along the direction of the major axe, the other is coarsening in three direction and combination with the other particles.

(4)The mean R is larger for the fracture surface than for the cross-section. The coarsened carbide particles cause SR embrittlement.

(5)Long elliptical particle is cut into small pieces by the fracture of specimen. This small pieces will prepare the site at which the cleavage fracture.

The authors wish to thank Dr. Jippei. Suzuki, Professor. of Mie University for his useful suggestions and Mr. Kazumasa. Miura, the student of Mie University for their cooperation to this research.

References

[1]Japan Welding Society: Yousetsu-Setugo Binran, (1990), 917.

[2]L.D. Jaffe, D.C. Buffum: Upper nose temper embrittlement of a Ni-Cr steel, Trans. AIME., 209-1(1957), 8-16.

[3]J.P. Naylor, M. Guttman: Mechanism of upper temper embrittlement in Mn-Ni-Mo A533 gr. B steel, Metal Science, 15-10(1981), 433-411.

[4]R.G. Baker, J. Nutting: The tempering of 2 1/4Cr-1Mo steel after quenching and normalizing, Journal of the Iron and Steel Institute, July(1959), 257-268.

[5]K. Tamaki, H. Kawakami, J. Suzuki: Temper embrittlement in HAZ of Cr-Mo Steels,: Welding in the World, Vol.43, No.2(1999), 36-48.

[6]American Society for Metals: Metals Handbook, Vol.8(1973), 37-47.

[7]H. Tamura: Computer-Gazou-Syori Nyumon, (1984), 75-107.

[8]T. Sakuma, N. Watanabe, T. Nishizawa: Effect of alloying element on the coarsening behavior of cementite particles in ferrite, Trans. JIM, Vol.21, No.3(1980), 159.